

Effect of Laser Remelting on the Microstructure and Corrosion Resistance of Plasma Sprayed Fe-based Coating

JIANG Chaoping^{1,3}, WANG Junxing¹, HAN Jianjun², LU Yuan², XING Yazhe¹,
CHEN Yongnan¹, SONG Xuding³

(1. School of Materials Science and Engineering, Chang'an University, Xi'an 710064, China; 2. Xi'an Special Equipment Inspection Institute, Xi'an 710065, China; 3. Key Laboratory of Road Construction Technology and Equipment MOE, Chang'an University, Xi'an 710064, China)

Abstract: Fe-based amorphous and nanocrystalline coatings were fabricated by air plasma spraying. The coatings were further treated by laser remelting process to improve their microstructure and properties. The corrosion resistance of the as-sprayed and laser-remelted coatings in 3.5wt% NaCl and 1 mol/L HCl solutions was evaluated by electrochemical polarization analysis. It was found that laser-remelted coating appeared much denser than the as-sprayed coating. However, laser-remelted coating contains much more nanocrystalline grains than the as-sprayed coatings, resulting from the lower cooling rate in laser remelting process compared with plasma spraying process. Electrochemical polarization results indicated that the laser-remelted coating has great corrosion resistance than the as-sprayed coating because of its dense structure.

Key words: plasma spraying; coating; laser remelting; corrosion

1 Introduction

Amorphous and nanocrystalline materials have been received great attention due to their exhibiting attractive combinations of properties such as high strength/hardness and excellent wear/corrosion resistance as compared to the materials with conventional grain size^[1,2]. Singh *et al* found that the surface microstructure and composition played a crucial role in determining the surface dependent engineering properties like resistance to wear and corrosion^[3]. It was reported that the wear and corrosion resistance of crystalline material could be improved by depositing an amorphous coating on its surface^[4]. It is well known that the amorphous metallic materials can be obtained by rapid quenching technique. Therefore, several coating technologies with high cooling rate during processing, such as laser surface processing^[5], high velocity oxygen fuel spraying^[6], kinetic spraying^[7] and air plasma spraying, have been used to fabricate

amorphous metallic coatings. Compared with the synthesis methods mentioned above, air plasma spraying is considered as a simple, versatile, and efficient coating process method in both research and industry fields due to its ability to produce much denser, stronger, and cleaner coatings^[8].

However, the pores in as-sprayed coating are a typical feature. The corrosion of Fe-based amorphous coatings was prone to appear around pores^[9,10]. The porosity of coating fabricated by air plasma spraying is about 3%. Laser treatment techniques have been successfully employed to decrease the porosity of as-sprayed coatings. It was reported that amorphous and nanocrystalline composite coatings could be prepared by laser cladding and remelting techniques^[11]. The cooling rate of laser remelting process was normally about 103 K/s, and the critical cooling rate for the formation of the Ni-Fe-B-Si-Nb amorphous phase was about 233 K/s^[12,13]. Zhu *et al*^[14] stated that laser cladding technology was an alternative approach to produce amorphous coatings. They prepared Fe-Co-B-Si-Nb coatings on low carbon steel surface by high power laser cladding using $[(\text{Fe}_{0.5}\text{Co}_{0.5})_{0.75}\text{B}_{0.2}\text{Si}_{0.05}]_{95.7}\text{Nb}_{4.3}$ amorphous powder. They found that the fraction of amorphous phase in the cladded coatings increased with increasing scanning speed. Although many attempts have been made to

use laser cladding technology to fabricate amorphous coating, the percentage of amorphous phase keeps a low level. Compared to laser cladding, the extremely fast cooling rate in laser remelting is ideal to retain or develop non-equilibrium microstructure including extended solid solution with amorphous/glassy state on a chosen crystalline substrate. Snezhnoi *et al*^[15] were the first to report the presence of an amorphous phase on the laser remelted chilled (ledeburitic) cast iron surface showing an average hardness of 1200 HV. Therefore, the laser remelting is believed to be a promising technology to enhance amorphous phase fraction and remove porosity defects of coatings.

In this work, the effects of laser remelting on the microstructure, phase composition and the corrosion resistance of the as-sprayed and laser-remelted coatings were investigated.

2 Experimental

2.1 Materials

Fe-based metallic alloy powder (Beijing SunSpraying Technology Co., Ltd., China) was used as the feedstock material. The Fe-based powder was prepared by gas atomization in the argon atmosphere after the master alloy was melted by a medium frequency vacuum induction furnace and passed through 160 mesh screen. The composition of Fe-based powder is listed in Table 1.

Table 1 Compositions of Fe-base powders

Element	Mo	Cr	Ni	P	Si	B	C	Fe
wt%	3.4	7.3	2.63	6.34	2.41	0.82	3.84	Bal.

2.2 Spraying process

Fe-based coatings were deposited on sand-blasted 45 steel plate (30 mm×15 mm×3 mm) surface by atmospheric plasma spraying. A GP -80 atmospheric air plasma spraying system was used to spray the coatings with a thickness of about 300 μm. Argon was used as primary gas, and hydrogen was used as auxiliary gas. The pressures of both argon and hydrogen were operated at 0.7 and 0.68 MPa, respectively, during spraying. The flow of the primary gas was fixed at 60 L/min, and that of the auxiliary gas was fixed at 6 L/min. Argon was used as powder feed gas and powder feed rate was 10 g/min. Plasma jet was operated to deposit the coatings at a power level of 25 kW (500A/50V).

2.3 Laser processing

After spraying the as-sprayed coatings were

remelted quickly by laser system (HWLW-300A). A high scanning speed of 8000 mm/min was used to remelt the coating under a power of 2 kW. The parameters could give a broad width and a deep depth of remelted layer and lead to a high cooling rate in the remelted layer. During the laser processing, a continuous flow of argon gas was maintained to prevent oxidation of the molten pool.

2.4 Characterization

The microstructure of the coatings after plasma spraying and laser remelting was characterized by scanning electron microscopy (SEM, S-4800). The phase compositions of the powder and coating were analyzed by X-ray diffraction (XRD, D/max 2500PC, Rigaku, Japan) with Cu K α radiation ($\lambda=1.5418 \text{ \AA}$) in the range of 20°-80° (2θ). Prior to potentiodynamic polarization test, the surfaces of as-sprayed coating and laser remelted coating were ground with silicon carbide papers and polished with 0.5 μm diamond pastes, followed by ultrasonic cleaning in acetone, washing in distilled water, and drying in air. The samples for the corrosion test were closely sealed with epoxy resin, leaving only an end-surface (with a surface area of 1 cm²) exposed for testing. The potentiodynamic polarization experiments were performed at room temperature in 3.5wt% NaCl and 1 mol/L HCl solutions, respectively.

3 Results and discussion

3.1 Structure and morphology of the coatings

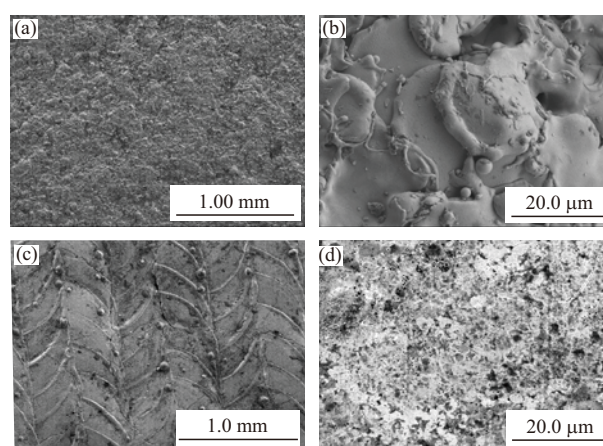


Fig.1 Surface SEM images of the coatings fabricated by plasma spraying(a,b) and laser remelting(c,d)

Fig.1 shows the surface morphologies of the as-sprayed and the laser-remelted coatings. As shown in Figs.1(a) and 1(b), there exist lots of pores on the surface of as-sprayed coating fabricated by plasma

spraying. This is the typical structure of plasma-sprayed coating due to the overlapping of flattened splats. Our previous studies confirmed that pores went against the formation and repair of the passive film^[16]. Figs.1(c) and 1(d) are the topography of the laser-remelted coating. It clearly shows the strip of laser scanning tracks and the effect of intense combination between the tracks. The scanning tracks present a peculiar fishbone feature after laser melting treatment. There exists trench between two overlapped tracks, and also exists ridge on single track. Moreover, some small pores appear in the remelted coating, as shown in Fig.1(d). During the laser melting process, some gases were trapped into melting pool. With the temperature decreased, the gases released and left the paths in the coating. These paths are the pores observed in Fig.1(d).

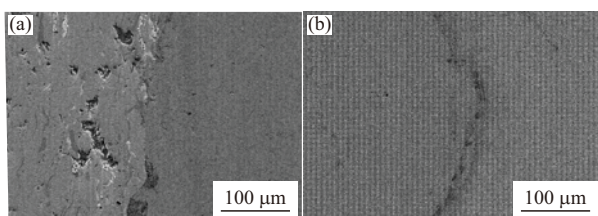


Fig. 2 Cross-sectional SEM images of (a) as-sprayed and (b) laser remelted coatings

Fig.2(a) presents the cross-sectional structure of Fe-based coatings prepared by air plasma spraying. Generally, all samples show typical lamellar structure in plasma sprayed coatings where the sprayed powders deformed and solidified when they impinged on the substrate surface to form splats. The splats piled up during spraying to gain the coating thickness. Many pores and in-plane microcracks exist in Fe-based coatings. Fig.2(b) shows the cross-sectional SEM images of the laser remelted coating near the top surface. After the laser remelting, a melting depth of 250 μm could be observed in the coatings. Compared with Fig.2(a), it can be seen that laser remelting changes the microstructure of the coating dramatically. There are no lamellar structure and fewer pores in the laser remelted coating.

Fig.3 shows XRD patterns of the as-sprayed and laser remelted coating. With the coating prepared by plasma spraying, the XRD pattern shows a broad halo peak at a diffraction angle of 44.8° (2θ), which is a typical characteristic of an amorphous structure. However, the pattern of laser remelted coating shows some sharp peaks, which means that crystals are also formed in the remelted layer. The crystalline peaks are identified as Fe_2B phase and body centered cubic $\alpha\text{-Fe}$ phase.

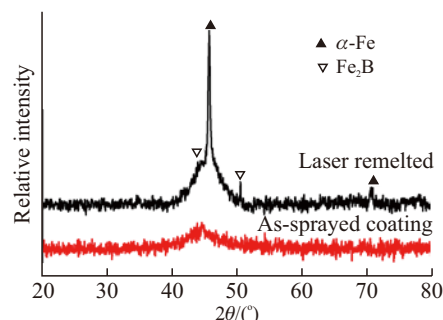


Fig.3 XRD patterns of as-sprayed and laser remelted coating

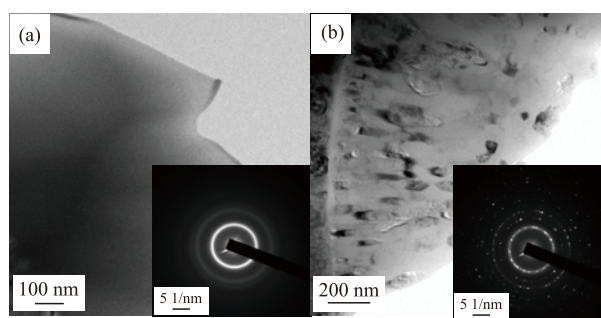


Fig.4 TEM images and selected area electron diffraction patterns of (a) as-sprayed and (b) laser remelted coating

TEM analysis was undertaken to obtain more detailed information on microstructure formation of the Fe-based coatings. Fig.4 gives the bright field electron micrographs and corresponding selected area electron diffraction (SAED) patterns of the coatings. For the main area of Fe-based coating, SAED pattern shows a diffuse ring, demonstrating the characteristic of the amorphous phase, as shown in Fig.4(a). Some nanocrystalline grains with average size of about 30 nm appear in local areas of laser remelted coating, as shown in Fig.4(b). The SAED pattern shows a diffuse ring and some diffraction spots.

3.2 Corrosion resistance

The polarization curves for the as-sprayed and laser remelted coatings in NaCl and HCl solutions are presented in Fig.5. There are some differences between the two processes in either curve shapes or current densities. As shown in Fig.5(a), corrosion potentials exhibit a difference of about 170 mV, which demonstrates that laser treated samples are not easy to corrode with less defects and high density. The laser remelted samples in HCl solution has the same corrosion behavior, as shown in Fig.5(b). The difference lays in that the corrosion potentials of as-sprayed coating and remelted coating exhibit a difference of about 73 mV. The laser-remelted coating is more inclined to corrosion in HCl solution than in NaCl solution.

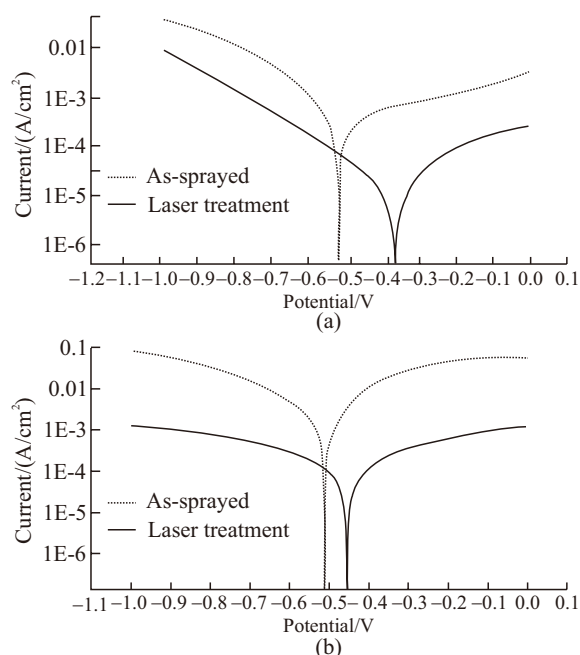


Fig.5 Potentiodynamic polarization curves of both as-sprayed and laser remelted coatings in 3.5wt% NaCl (a) and in 1 mol/L HCl Solution (b)

Table 2 Corrosion potentials and polarization current densities of the coatings

Solution	Sample	Corrosion potential /V	Current density /($\mu\text{A}\cdot\text{cm}^{-2}$)
3.5% NaCl	As-sprayed	-0.525	109
	Laser treated	-0.355	5
1 mol/L HCl	As-sprayed	-0.524	688
	Laser treated	-0.451	39.4

The corrosion current density (i_{corr}) values estimated by Tafel extrapolation method are listed in Table 2. The corrosion current densities of laser remelted samples in NaCl and HCl are 5 and 39.4 $\text{A}\cdot\text{cm}^{-2}$, respectively. Compared with the as-sprayed sample, a marked decrease in corrosion current density for the laser remelted sample can be found, indicating the beneficial remelting process. As for the as-sprayed sample, plenty of pores provide extra reaction area, resulting in poor corrosion resistance. After the laser remelting, most of the pores are eliminated and a dense structure forms. As a result, real reaction area is decreased significantly and the corrosion resistance is enhanced accordingly.

4 Conclusions

Laser remelting was applied in surface treatment of Fe-based amorphous and nanocrystalline coatings fabricated by air plasma spraying. The microstructure of the coatings changes with laser remelting treatment. The laser remelting influences not only the amount of

amorphous phase, but also the shape and distribution of the crystallization grains. The polarization curves for the as-sprayed and laser remelted coatings confirm that the laser remelting can improve the corrosion resistance of plasma-sprayed Fe-based amorphous and nanocrystalline coatings in NaCl and HCl solutions. Though the amount of amorphous phase is reduced during laser remelting process, the dense structure resulted from laser remelting plays an important role in the enhancement of the corrosion performance.

References

- [1] Inoue, Shen B, Nishiyama N. Bulk Metallic Glasses [J]. *Springer*, 2008:1-25
- [2] Inoue, Shen B, Takeuchi A. Developments and Applications of Bulk Glassy Alloys in Late Transition Metal Base System [J]. *Mater. Trans.*, 2006, 47: 1 275-1 285
- [3] Singh A, Bakshi S, Agarwal A, *et al.* Microstructure and Tribological Behavior of Spark Plasma Sintered Iron-based Amorphous Coatings[J]. *Mater. Sci. Eng., A*, 2010, 527: 5 000-5 007
- [4] Nicolas S, Francoise H, Sophie C, *et al.* Corrosion Properties of *in Situ* Laser Remelted NiCrBSi Coatings Comparison with Hard Chromium Coatings [J]. *J. Mater. Process. Technol.*, 2011, 211:133-140
- [5] Basu A, Sarnant AN, Harimkar SP, *et al.* Laser Surface Coating of Fe-Cr-Mo-Y-B-C Bulk Metallic Glass Composition on AISI 4041 Steel [J]. *Surf. Coat. Technol.*, 2008, 202: 2 623-2 631
- [6] Guo RQ, Zhang C, Chen Q, *et al.* Study of Structure and Corrosion Resistance of Fe-based Amorphous Coatings Prepared by HVOF and HVOF [J]. *Corros. Sci.*, 2011, 53: 2 351-2 356
- [7] Yoon S, Bae G, Xiong Y, *et al.* Strain-enhanced Nanocrystallization of a CuNiTiZr Bulk Metallic Glass Coating by a Kinetic Spraying Process [J]. *Acta Mater.*, 2009, 57: 6 191-6 199
- [8] Huang YJ, Guo YZ, Fan HB, *et al.* Synthesis of Fe-Cr-Mo-C-B Amorphous Coating with High Corrosion Resistance[J]. *Mater. Lett.*, 2012, 89: 229-232
- [9] Zhou Z, Wang L, Wang FC, *et al.* Formation and Corrosion Behavior of Fe-based Amorphous Metallic Coatings by HVOF Thermal Spraying [J]. *Surf. Coat. Technol.*, 2009, 204: 563-570
- [10] Wang Y, Zheng YG, Ke W, *et al.* Slurry Erosion-corrosion Behaviour of High-velocity Oxy-fuel (HVOF) Sprayed Fe-based Amorphous Metallic Coatings for Marine Pump in Sand-containing NaCl Solutions [J]. *Corros. Sci.*, 2011, 53:3177-3185
- [11] Zhang PL, Yan H, Yao CW, *et al.* Synthesis of Fe-Ni-B-Si-Nb Amorphous and Crystalline Composite Coatings by Laser Cladding and Remelting [J]. *Surf. Coat. Technol.*, 2011, 206: 1 229-1 236
- [12] Shen BL, Chang CT, Inoue A. Ni-based Bulk Glassy Alloys with Superhigh Strength of 3800 MPa in Ni-Fe-B-Si-Nb System [J]. *Appl. Phys. Lett.*, 2006, 88:201 903-201 906
- [13] Li RF, Li ZG, Huang J, *et al.* Dilution Effect on the Formation of Amorphous Phase in the Laser Cladded Ni-Fe-B-Si-Nb Coatings after Laser Remelting Process [J]. *Appl. Surf. Sci.*, 2012, 258: 7 956-7 961
- [14] Zhu YY, Li ZG, Huang J, *et al.* Amorphous Structure Evolution of High Power Diode Laser Cladded Fe-Co-B-Si-Nb Coatings [J]. *Appl. Surf. Sci.*, 2012, 261: 896-901
- [15] Wu XL, Hong YS. Fe-based Thick Amorphous-alloy Coating by Laser Cladding [J]. *Surf. Coat. Technol.*, 2001, 141(2/3): 141-144
- [16] Jiang CP, Xing YZ, Zhang FY, *et al.* Microstructure and Corrosion Resistance of Fe/Mo Composite Amorphous Coatings Prepared by Air Plasma Spraying [J]. *Int. J. Mine. Mater.*, 2012, 19: 657-662